Orientational twins in an improper ferroelastic phase transition driven by the M_5^- zone-boundary phonon in $R\mathrm{Ag}_{1-x}\mathrm{In}_x$

Dorian M. Hatch,[1] Wenwu Cao,[2] and Avadh Saxena[3]
[1]*Department of Physics, Brigham Young University, Provo, Utah 84602*
[2]*Department of Mathematics and Materials Research Laboratory, The Pennsylvania State University, University Park, Pennsylvania 16802*
[3]*Theoretical Division, Los Alamos National Laboratory, Los Alamos, New Mexico 87545*
(Received 30 March 2001; published 14 February 2002)

Orientational twins involve two domain states that exhibit rotational symmetry relationships between them. For an improper ferroelastic cubic to tetragonal first-order phase transition driven by the M_5^- zone-boundary phonon in the CsCl structure, there are three possible directions for the tetragonal axis of the low-temperature phases. The existence of four antiphase-related-domain states for each given tetragonal orientation introduces additional possible pairing schemes for the twins. We obtain only three distinct domain pair classes: two antiphase boundary classes and one orientational boundary class. For this O_h^1-D_{4h}^{17} ($Pm\bar{3}m$-I4/mmm) transition we derive the general governing equations for the orientational twins based on a Ginzburg-Landau theory, which constitute a system of four coupled nonlinear differential equations. General features of the orientational twin solutions are demonstrated through a special choice of the parameters for which the four coupled equations can be reduced to two. The orientational twin boundaries have relatively large elastic energy and, therefore, they are strongly restricted to preferred lattice planes.

DOI: 10.1103/PhysRevB.65.094110 PACS number(s): 64.70.Kb, 02.20.−a, 61.50.Ah, 61.50.Ks

I. INTRODUCTION

The O_h^1 ($Pm\bar{3}m$) to D_{4h}^{17}(I4/mmm) cubic to tetragonal improper ferroelastic first-order phase transition in $R\mathrm{Ag}_{1-x}\mathrm{In}_x$ (where R=La, Ce, and Pr) results in 12 different domain states with three independent tetragonal axes. As discussed in Ref. 1 there are four different displacement patterns for each tetragonal axis, which differ by a fractional translation of the parent unit cell. These four domain states with the same tetragonal axis can form antiphase structures. An antiphase pair is a domain pair relationship where a pure lattice translation is lost from the parent symmetry group and transforms the first domain into the second. Another important type of domain structure is an orientational pair, which is commonly referred to as a ''twin.'' An orientational twin boundary (OTB) is formed by two domains that are related by a lost rotation from the parent group but that cannot be related by a pure translation. The orientational twins considered here consist of two domain states having different tetragonal axes. The domain walls tend to be planar since the elastic energy is high for wall bending. In addition, the number of orientations for the twin domain pair walls are more limited than for antiphase boundaries.

The study of various types of domain walls and their energetics in the context of both the first- and second-order structural phase transitions has been carried out in recent years for a variety of materials. Within the Ginzburg-Landau formalism a few analytic solutions for these domain walls have been obtained for relatively simple free energy functionals. However, it becomes an increasingly unwieldy task to classify and study all possible domain walls when (i) the primary and/or secondary order parameters are multicomponent, and (ii) there are several independent invariants in the gradient (Ginzburg) part of the free energy.

We illustrate a general approach to these considerations in the context of ferroic phase transitions occurring in materials with CsCl structure (space group O_h^1,$Pm\bar{3}m$) induced by M_5^- mode softening, specifically, a first order, improper ferroelastic transition to a tetragonally distorted low symmetry phase (D_{4h}^{17},I4/mmm), such as in the pseudobinary rare-earth alloy $\mathrm{LaAg}_{1-x}\mathrm{In}_x$ ($x\sim0.2$) (Fig. 1(a)). We have previously identified the six-component primary order parameter (OP), nineteen secondary OP's (including strain), and presented the Landau free energy.[2] In addition, we found five gradient invariants[3] for the M_5^- distortion mode. The class of OP directions consistent with this irreducible representation and the observed atomic displacements of the rare-earth alloy is denoted as P_{10} in the notation of Stokes and Hatch[4] and contains 12 equivalent directions (or domains).

Note that the scientific and technological interest in the CsCl structure materials is related to the tendency of the transverse acoustic (TA) phonon mode to soften at the M point of the Brillouin zone. For $\mathrm{LaAg}_{1-x}\mathrm{In}_x$ ($x=0.2$) the structure has been determined and softening of both the shear modulus and the TA (Σ_2) phonon mode at the M point have been observed. In addition to $R\mathrm{Ag}_{1-x}\mathrm{In}_x$, there are related materials, e.g., YCu and LaCd, that undergo similar cubic to tetragonal transformations. The cubic to orthorhombic transition caused by a related M-point phonon softening observed in the shape memory alloys AuCd and NiTi-M (M =Fe, Al, Cu) (Refs. 5–7) can be understood within the present Ginzburg-Landau free-energy (GLFE) framework. Therefore, the results on the orientational twin boundary presented here have a wide applicability.

In this paper we present a systematic and comprehensive group-theoretic treatment of domain walls based on the concepts of the *direction* of the OP and the *isotropy group* of the OP.[4] For a given phase transition, this technique allows us to

 ©2002 The American Physical Society

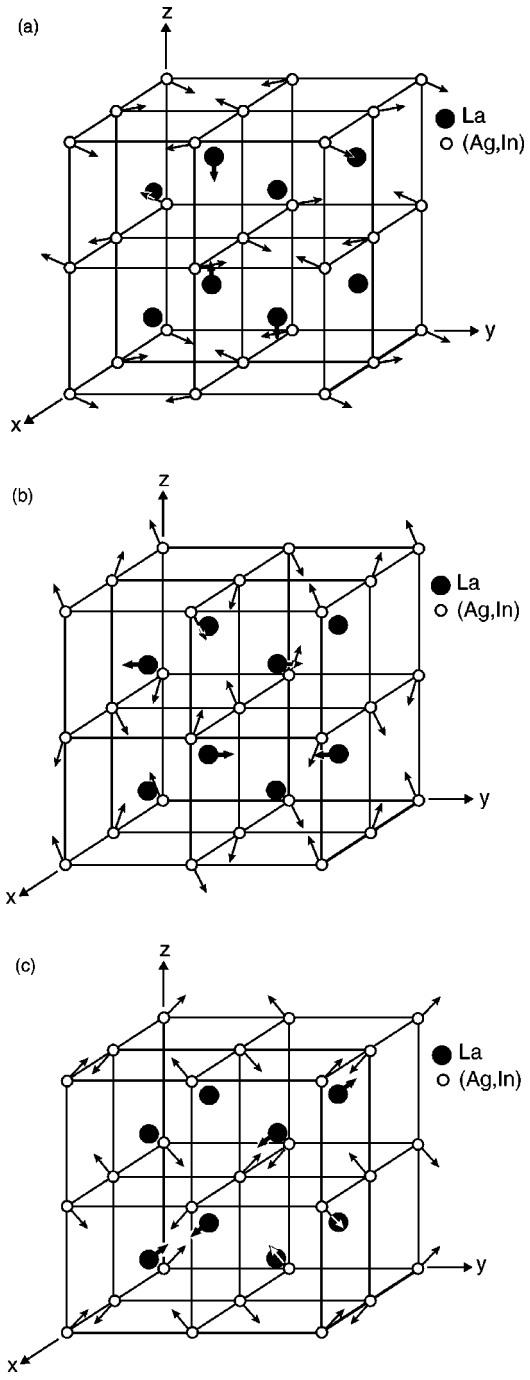

FIG. 1. Three different domain states of CsCl structure with displacements of M_5^- symmetry that lead for $R\mathrm{Ag}_{1-x}\mathrm{In}_x$ to a D_{4h}^{17} tetragonal low-temperature structure.

(a) construct all independent (Landau) free-energy and gradient invariants, (b) classify possible homogeneous phases, (c) classify all crystallographically equivalent domains and domain pairs, (d) obtain criteria for the stability, merging, and splitting of domain walls, (e) determine secondary OP's and their effect on the domain walls, and finally (f) calculate the continuous OP profiles for (antiphase and) orientational twin structures. This procedure could be widely applied to ferromagnetic, ferroelectric, ferroelastic, magnetoelastic, (perovskite based) high-T_c superconductors and colossal-magnetoresistance materials, pseudobinary rare earth alloys (e.g., $R\mathrm{Ag}_{1-x}\mathrm{In}_x$, $R=$La, Ce, Pr) and many other materials.

Based on the same model as in Ref. 1, in the following two sections, we address in detail the problem of domain pairs and orientational twins, respectively, from a group-theoretical perspective. In Sec. II we analyze domain pairs. We find *only one* crystallographically distinct class of OTB's and *two* distinct classes of antiphase boundaries (APB) out of $(\frac{1}{2})(12)(13)=78$ possible boundaries. The APB's were studied in detail in Ref. 1. Here we emphasize OTB's. In Sec. III the (solitonlike) OP profiles for a twin domain are computed and the constraints on the free-energy coefficients are determined for the specific OTB. For more general cases, we present a set of four coupled nonlinear differential equations and look at some special twin solutions and corresponding lattice displacements. We summarize the main results in Sec. IV. The details of the variational equations are given in the Appendix.

II. DOMAIN PAIRS

Possible homogeneous crystal structures are obtained by minimization of the Landau part of the GLFE. From these solutions one finds the values of the order parameters, which are then used as boundary conditions for the heterogeneous problems. In our case, the high symmetry is O_h^1 $(Pm\bar{3}m)$, and the lower symmetry is $D_{4h}^{17}(\mathrm{I}4/mmm)$. The M_5^- irreducible representation of the O_h^1 cubic space group is the representation of interest here. This representation defines three arms of the star, corresponding to the points $(2\pi/a)\times(\frac{1}{2},\frac{1}{2},0)$, $(2\pi/a)(\frac{1}{2},0,\frac{1}{2})$ and $(2\pi/a)(0,\frac{1}{2},\frac{1}{2})$ in the Brillouin zone and two-dimensional small representations.[8] The *class* of OP directions P_{10} defined in Ref. 4 gives us the correct distortions at the transition and the representative expression for the OP (domain 1) is $\boldsymbol{\eta}=(a,a,0,0,a,-a)$, where a is an arbitrary lattice mode displacement amplitude. Thus the P_{10} direction combines contributions from two arms of the star, arms 1 and 3 for this domain. The elements of the isotropy subgroup D_{4h}^{17} for this order-parameter direction are listed in Table I, and have a point group of order 16.

This is not the most general orientation of the OP. Corresponding to the most general direction, $6D1^4$, the triclinic subgroup $C_1^1(P1)$ with a cell size change of 4 is obtained. Nor is this the highest possible symmetry for this IR, since the direction $(a,0,0,0,0,0)$, corresponding to one arm of the star, gives the orthorhombic space group $D_{2h}^5(Pmma)$ with only a size change of 2. However, the particular transition of interest here defines the choice of the order-parameter direction P_{10}.

There are 12 equivalent domains (or directions) for the P_{10} class[4,9] that correspond to the minimization of this GLFE. Each domain can be obtained from another domain by a lost high-symmetry operation.[10] We denote these directions as $P_{10}(i)$ with $i=1,...,12$. Any domain can be chosen as a representative for the class. These crystallographically equivalent domains constitute a distinct orbit[11] with respect to the space group G_0 (O_h^1 for our specific considerations). Two domains are *crystallographically equivalent*, i.e., they

TABLE I. Elements of isotropy subgroup I4/mmm, domain 1.

Basis vectors	Origin	Elements
(2,0,0), (0,2,0), (0,0,2)	$(\frac{1}{2},\frac{1}{2},0)$	$(E\|0,0,0)$, $(C_{2x}\|0,1,0)$, $(C_{2y}\|1,0,0)$, $(C_{2z}\|1,1,0)$, $(C_{2b}\|1,1,0)$, $(C_{4z}+\|1,0,0)$, $(C_{4z}^{-}\|0,1,0)$, $(C_{2a}\|0,0,0)$, $(\mathrm{I}\|1,1,0)$, $(\sigma_x\|1,0,0)$, $(\sigma_y\|0,1,0)$, $(\sigma_x\|0,0,0)$, $(\sigma_{db}\|0,0,0)$,$(S_{4z}^{-}\|0,1,0)$, $(S_{4z}^{+}\|1,0,0)$, $(\sigma_{da}\|1,1,0)$

have the same structure but different orientations or positions, if there is an element, g in G_0, that can transform one domain into the other. For our case this means, if g is in O_h^1 then $gP_{10}(i)=P_{10}(j)$. All such domains can be obtained by acting with the operations of O_h^1 on the OP expression for any one domain, say $P_{10}(1)$. The resulting set constitutes a *class* of crystallographically equivalent domains.

The group elements that do not change (i.e., leave invariant) the order parameter, for a particular domain, form the *isotropy group* F of OP direction. F must be a subgroup of O_h^1. For direction P_{10}, domain one, the subgroup is D_{4h}^{17} with the specific symmetry elements listed in Table I. The other equivalent order-parameter directions are listed in Table II and are denoted 1 through 12 in column two. In Table II we give the OP directions in the equivalent labeling corresponding to lattice normal modes $\mathbf{Q}$.[1,2] The normal-mode basis $\mathbf{Q}$ is related to the order-parameter basis (denoted by $\boldsymbol{\eta}$) through an orthogonal transformation. In column 5 of Table II we list the displacements arising from the M_5^- mode inducing the transition to the subgroup D_{4h}^{17}. We have listed the displacements of the atoms, which are in equivalent in the body-centered tetragonal subgroup. Their positions and directions are indicated with respect to the cubic O_h^1 axes. All other atoms in the D_{4h}^{17} structure can be obtained by lattice

TABLE II. Order parameter directions: Homogeneous solutions.

Tetragonal axis	Label	State	Order parameter Q, η	Displacement at $x,y,z=[0,0,0]$, $[1,0,0]$, $[0,1,0]$, $[0,0,1]$ at $x,y,z,=1/2[1,1,1]$, $1/2[3,1,1]$, $1/2[1,3,1]$, $1/2[1,1,3]$
x	3	I_x	$(0,Q_0,Q_0,0,0,0)$ $(a,-a,a,a,0,0)$	$[011]$, $[0\bar{1}1]$, $[0\bar{1}\bar{1}]$, $[01\bar{1}]$ $[100]$, $[\bar{1}00]$, $[000]$, $[000]$
	6	II_x	$(0,-Q_0,Q_0,0,0,0)$ $(a,-a,-a,-a,0,0)$	$[0\bar{1}1]$, $[01\bar{1}]$, $[011]$, $[0\bar{1}\bar{1}]$ $[000]$, $[000]$, $[100]$, $[\bar{1}00]$
	9	III_x	$(0,Q_0,-Q_0,0,0,0)$ $(-a,a,a,a,0,0)$	$[01\bar{1}]$, $[0\bar{1}1]$, $[0\bar{1}\bar{1}]$, $[011]$ $[000]$, $[000]$, $[\bar{1}00]$, $[100]$
	12	IV_x	$(0,-Q_0,-Q_0,0,0,0)$ $(-a,a,-a,-a,0,0)$	$[0\bar{1}\bar{1}]$, $[011]$, $[01\bar{1}]$, $[0\bar{1}1]$ $[\bar{1}00]$, $[100]$, $[000]$, $[000]$
y	2	I_y	$(Q_0,0,0,0,0,Q_0)$ $(0,0,a,-a,a,a)$	$[101]$, $[\bar{1}01]$, $[\bar{1},0,\bar{1}]$, $[10\bar{1}]$ $[010]$, $[000]$, $[0\bar{1}0]$, $[000]$
	5	II_y	$(Q_0,0,0,0,0,-Q_0)$ $(0,0,a,-a,-a,-a)$	$[10\bar{1}]$, $[\bar{1}0\bar{1}]$, $[\bar{1}01]$, $[010]$ $[000]$, $[0\bar{1}0]$, $[000]$, $[010]$
	8	III_y	$(-Q_0,0,0,0,0,Q_0)$ $(0,0,-a,a,a,a)$	$[\bar{1}01]$, $[101]$, $[10\bar{1}]$, $[\bar{1}0\bar{1}]$ $[000]$, $[010]$, $[000]$, $[0\bar{1}0]$
	11	IV_y	$(-Q_0,0,0,0,0,-Q_0)$ $(0,0,-a,a,-a,-a)$	$[\bar{1}0\bar{1}]$, $[10\bar{1}]$, $[101]$, $[\bar{1}01]$ $[0\bar{1}0]$, $[000]$, $[010]$, $[000]$
z	1	I_z	$(0,0,0,Q_0,Q_0,0)$ $(a,a,0,0,a,-a)$	$[110]$, $[\bar{1}10]$, $[1\bar{1},0,]$, $[\bar{1}\bar{1}0]$ $[001]$, $[000]$, $[000]$, $[00\bar{1}]$
	4	II_z	$(0,0,0,-Q_0,Q_0,0)$ $(-a,-a,0,0,a,-a)$	$[\bar{1}\bar{1}0]$, $[110]$, $[\bar{1}10]$, $[1\bar{1}0]$ $[000]$, $[001]$, $[00\bar{1}]$, $[000]$
	7	III_z	$(0,0,0,Q_0,-Q_0,0)$ $(a,a,0,0,-a,a)$	$[1\bar{1}0]$, $[\bar{1}10]$, $[110]$, $[\bar{1}\bar{1}0]$ $[000]$, $[00\bar{1}]$, $[001]$, $[000]$
	10	IV_z	$(0,0,0,-Q_0,-Q_0,0)$ $(-a,-a,0,0,-a,a)$	$[\bar{1}00]$, $[1\bar{1}0]$, $[\bar{1}\bar{1}0]$, $[110]$ $[00\bar{1}]$, $[000]$, $[000]$, $[001]$

translations and body centering within the subgroup, e.g., lattice translations (2,0,0,), (0,2,0), (0,0,2) and body centering position $(\frac{1}{2}, \frac{1}{2}, \frac{1}{2})$ for domain 1.

If a group operation t_{i1} transforms domain 1 into domain i, $t_{i1}d(1)=d(i)$, then all the elements of the left coset $t_{i1}F^{(1)}$ also transform domain one into domain i

$$t_{i1}F^{(1)}d(1)=t_{i1}d(1)=d(i),$$

where $F^{(1)}$ is the isotropy group of domain one. There are twelve sets of distinct elements $t_{i1}F^{(1)}$ that will transform $d(1)$ into $d(i)$, $i=1,2,3,...,12$, respectively. In fact the parent group O_h^1 can be decomposed into left cosets:[11]

$$G_0=EF^{(1)}+t_{2,1}F^{(1)}+\cdots+t_{12,1}F^{(1)}. \quad (1)$$

The ith left coset transforms domain 1 into domain i. Eleven left cosets are listed in Table III while the first left coset is just the isotropy group $F^{(1)}$, or D_{4h}^{17}, with the elements listed in Table I.

An ordered pair of domains is written as $(P(i),P(j))$. The set of transformations t_{ji} such that $t_{ji}P(i)=P(j)$ is labeled T_{ji}. The two domain pairs $(P(i),P(j))$, and $(P(k),P(l))$ are said to be *crystallographically equivalent* to each other if there exists an element of O_h^1 such that $gP(i)=P(k)$, and simultaneously $gP(j)=P(l)$. We denote this equivalency as $(P(i),P(j))\sim(P(k),P(l))$. All such equivalent domain pairs form a *domain pair class*. Domain pair classes can be determined by the decomposition of O_h^1 into *disjoint double cosets*.[11–13]

$$G_0=F^{(i)}cF^{(i)}+F^{(i)}t_{2i}F^{i}+\cdots+F^{(i)}t_{r1}F^{(i)}.$$

Each double coset corresponds to the following action: the left coset $t_{ri}F^{(i)}$ above transforms domain $P(i)$ into $P(r)$. If we then act with an element g of $F^{(i)}$ on the domain pair $(P(i),P(r))$ an equivalent domain pair is obtained, namely, $(P(i),gP(r))=(P(i),gt_{ri}F^{(i)}P(i))$. All such pairs for g in $F^{(i)}$ are crystallographically equivalent to $(P(i),P(r))$. Thus the number of inequivalent domain pairs is in one-to-one correspondence with the usual double coset process of group theory. The concept of a domain pair class is important since domain pairs belonging to the same class will have equivalent relative symmetry properties, differing only in their orientation relative to the parent group. Therefore, we need only consider a representative domain pair that belongs to that class. We pick the representative pair so that $P(1)$ is always in the first position, i.e., of the form $(P(1),P(j))$. This representative domain pair then yields the types of domain walls to be investigated, which are common to all pairs in this class.

Antiphase domains imply a domain relationship where a pure translation can be found in the left coset that transforms the first domain into the second. *Twin* domains cannot be related by a pure translation, but by (proper or improper) rotations or, for nonsymmorphic space groups, by rotations together with translations. For the O_h^1 to D_{4h}^{17} transition we obtain two distinct classes of antiphase pairs represented by the pairs (1,4) and (1,10), which were studied in detail in Ref. 1 and we will not consider them further here. (We have dropped the P_{10} notation from the domain labeling since we are now restricting our attention to just this class of OP directions.) We obtain only one class of OTB's represented by (1,2). Other equivalently related domain pairs in these three classes are given in Table IV. We stress that the group-theoretical methods used here are systematic and have effectively reduced our considerations to only three domain pair types represented by the domain pairs (1,4) (1,10), and (1,2) rather than the 78 possible pairs that might initially be considered. We dropped consideration of the trivial fourth domain pair class corresponding to the pair (1,1).

Every domain has definite values for *secondary* OP's, O_j. A secondary OP is a parameter direction from another IR of the high symmetry group, which is also invariant under the symmetry group of the primary OP, i.e., $F^{(i)}O_j=O_j$. Since the symmetry of the lower symmetry phase is a subgroup of the parent phase, the isotropy group of O_j can be a supergroup of $F^{(i)}$ (and must be a subgroup of G_0). From these group symmetries we can find the corresponding physical distortions that can be chosen as secondary OP's. The secondary OP of interest here is the spontaneous strain. In a ferroelastic crystal, the domain wall direction(s) is(are) along some specific direction(s).[14,15] e.g., $y=\pm z$ defines the domain walls for domains 1 and 2.

III. ORIENTATIONAL TWINS

We have collected the 12 domains, listed in Table II, into three sets corresponding to the three possible directions for the tetragonal orientation. The four domain states in each tetragonal orientation are antiphase related and we represent them by Roman numerals I–IV. The tetragonal axis is labeled by a subscript x, y, or z. For example, I_x represents domain state I with tetragonal axis in the x direction. We choose domain states I_x and I_y, corresponding to an orientational twin, as an example to derive the equations for equilibrium configurations. The displacement patterns for these two domains are shown in Figs. 1(b) and 1(c). This orientational twin is equivalent to the (1,2) twin representative.

From the results of Sapriel[15] the wall orientations for ferroelastic twins are determined by strain compatibility conditions. These wall orientations minimize elastic strain energies. For the twins between domain states I_x and I_y, one of the allowed domain walls has its normal in $[1\bar{1}0]$. In the discussion presented below, we will assume this domain wall orientation to illustrate the use of the Ginzburg-Landau theory to derive the OTB structure profile.

The order-parameter ''vector'' has four nonzero components. (For an antiphase boundary, only two components are nonzero, see Ref. 1). The free energy for the I_x-I_y orientational twin can be written as follows:

$$F=F_L+F_{el}+F_c+F_G, \quad (2)$$

where (setting, $Q_4=Q_5=0$ in the free-energy expression in Refs. 1 and 2).

TABLE III. Left cosets relative to D_{4h}^{17} of domain 1.

T1,I	Operations
$T_{2,1}$	$\{C_{31-}\|000\}$, $\{S_{61+}\|010\}$, $\{C_{34-}\|100\}$, $\{S_{64+}\|001\}$, $\{C_{32-}\|001\}$, $\{S_{62+}\|100\}$, $\{C_{33-}\|010\}$, $\{S_{63-}\|000\}$, $\{C_{4x+}\|000\}$, $\{S_{4x-}\|010\}$, $\{C_{2f}\|010\}$, $\{\sigma_{df}\|000\}$, $\{C_{4x-}\|001\}$, $\{S_{4x+}\|100\}$, $\{C_{2d}\|100\}$, $\{\sigma_{dd}\|001\}$
$T_{3,1}$	$\{C_{31+}\|000\}$, $\{S_{61-}\|100\}$, $\{C_{32+}\|001\}$, $\{S_{62-}\|010\}$, $\{C_{33+}\|010\}$,$\{S_{63-}\|001\}$, $\{C_{34+}\|100\}$, $\{S_{64-}\|000\}$, $\{C_{4y-}\|000\}$, $\{S_{4y+}\|100\}$, $\{C_{2e}\|100\}$, $\{\sigma_{de}\|000\}$, $[C_{2c}\|010]$, $\{\sigma_{dc}\|001\}$, $\{C_{4y+}\|001\}$, $\{S_{4y-}\|010\}$
$T_{4,1}$	$\{C_{2y}\|000\}$, $\{\sigma_y\|001\}$, $\{C_{2z}\|010\}$, $\{\sigma_z\|100\}$, $\{E\|100\}$, $\{I\|010\}$, $\{C_{2x-}\|001\}$, $\{\sigma_z\|000\}$, $\{C_{4z+}\|000\}$, $\{S_{4z-}\|001\}$, $\{C_{4z-}\|001\}$, $\{S_{4z+}\|000\}$, $\{C_{2a}\|100\}$, $\{\sigma_{da}\|010\}$, $\{C_{2b}\|010\}$, $\{\sigma_{db}\|100\}$
$T_{5,1}$	$\{C_{32-}\|000\}$, $\{S_{62+}\|010\}$, $\{C_{33-}\|100\}$, $\{S_{63+}\|001\}$, $\{C_{31-}\|001\}$, $\{S_{61+}\|100\}$, $\{C_{34-}\|010\}$, $\{S_{64+}\|000\}$, $\{C_{4x-}\|000\}$, $\{S_{4x+}\|010\}$, $\{C_{2d}\|010\}$, $\{\sigma_{dd}\|000\}$, $\{C_{4x+}\|001\}$, $\{S_{4x-}\|100\}$, $\{C_{2f}\|100\}$, $\{\sigma_{df}\|001\}$
$T_{6,1}$	$\{C_{33+}\|000\}$, $\{S_{63-}\|100\}$, $\{C_{34+}\|001\}$, $\{S_{64}\|010\}$, $\{C_{31+}\|010\}$, $\{S_{61-}\|001\}$, $\{C_{32+}\|100\}$, $\{S_{62-}\|000\}$, $\{C_{2c}\|000\}$, $\{\sigma_{dc}\|100\}$, $\{S_{4y+}\|100\}$, $\{S_{4y-}\|000\}$, $\{C_{4y-}\|010\}$, $\{S_{4y+}\|001\}$, $\{C_{2e}\|001\}$, $\{\sigma_{de}\|010\}$
$T_{7,1}$	$\{C_{2x}\|000\}$, $\{\sigma_x\|001\}$, $\{E\|010\}$, $\{I\|100\}$, $\{C_{2x}\|100\}$, $\{\sigma_z\|010\}$, $\{C_{2y}\|001\}$, $\{\sigma_y\|000\}$, $\{C_{4z-}\|000\}$, $\{S_{4z+}\|001\}$, $\{C_{4z+}\|001\}$, $\{S_{4z-}\|000\}$, $\{C_{2b}\|100\}$, $\{\sigma_{db}\|010\}$, $\{C_{2a}\|010\}$, $\{\sigma_{da}\|100\}$
$T_{8,1}$	$\{C_{34-}\|000\}$, $\{S_{64+}\|010\}$, $\{C_{31-}\|100\}$, $\{S_{61+}\|001\}$, $\{C_{33-}\|001\}$, $\{S_{63+}\|100\}$, $\{C_{32-}\|010\}$, $\{S_{62+}\|000\}$, $\{C_{2d}\|000\}$, $\{\sigma_{dd}\|010\}$, $\{C_{4x-}\|010\}$, $\{S_{4x+}\|000\}$, $\{C_{2f}\|001\}$, $\{\sigma_{df}\|100\}$, $\{C_{4x+}\|100\}$, $\{S_{4x}\|001\}$
$T_{9,1}$	$\{C_{32+}\|000\}$, $\{S_{62-}\|100\}$, $\{C_{31+}\|001\}$, $\{S_{61-}\|010\}$, $\{C_{34+}\|010\}$, $\{S_{64-}\|001\}$, $\{C_{33+}\|100\}$, $\{S_{63-}\|010\}$, $\{C_{4y}\|000\}$, $\{S_{4y-}\|100\}$, $\{C_{2c}\|100\}$, $\{\sigma_{dc}\|000\}$, $\{C_{2e}\|010\}$, $\{\sigma_{de}\|001\}$, $\{C_{4y-}\|001\}$, $\{S_{4y+}\|001\}$
$T_{10,1}$	$\{C_{2z}\|000\}$, $\{\sigma_z\|001\}$, $\{C_{2y}\|010\}$, $\{\sigma_y\|100\}$, $\{C_{2x}\|100\}$, $\{\sigma_x\|010\}$, $\{E\|001\}$, $\{I\|000\}$, $\{C_{2b}\|000\}$, $\{\sigma_{db}\|001\}$, $\{C_{2a}\|001\}$, $\{\sigma_{da}\|000\}$, $\{C_{4z-}\|100\}$, $\{S_{4z+}\|010\}$, $\{C_{4z+}\|010\}$, $\{S_{4z-}\|100\}$
$T_{11,1}$	$\{C_{33-}\|000\}$, $\{S_{63+}\|010\}$, $\{C_{32-}\|100\}$, $\{S_{62+}\|001\}$, $\{C_{34-}\|001\}$, $\{S_{64+}\|100\}$, $\{C_{31-}\|010\}$, $\{S_{61+}\|000\}$, $\{C_{2f}\|000\}$, $\{\sigma_{df}\|010\}$, $\{C_{4x+}\|010\}$, $\{S_{4x-}\|000\}$, $\{C_{2d}\|001\}$, $\{\sigma_{dd}\|100\}$, $\{C_{4z-}\|100\}$, $\{S_{4x}\|001\}$
$T_{12,1}$	$\{C_{34+}\|000\}$, $\{S_{64-}\|100\}$, $\{C_{33+}\|001\}$, $\{S_{63-}\|010\}$, $\{C_{32+}\|010\}$, $\{S_{62-}\|001\}$, $\{C_{31+}\|100\}$, $\{S_{61-}\|000\}$, $\{C_{2e}\|000\}$, $\{\sigma_{de+}\|100\}$, $\{C_{4y-}\|100\}$, $\{S_{4y}\|000\}$, $\{C_{4y+}\|010\}$, $\{S_{4y+}\|001\}$, $\{C_{2c}\|001\}$, $\{\sigma_{dc}\|010\}$

TABLE IV. Equivalent domain paris. *k,m,n* are positive integers; $k+3m$, $k+3n+1$, $k+3n+2$ are smaller than 12. The domain pairs (1,10) and (1,4) are antiphase boundaries studied in Ref. 1 whereas (1,2) is the orientational twin boundary.

Domain pair type	Domain pairs
(1,10)	(2,11), (3,12), (4,7), (5,8), (6,9)
(1,4)	$(k,k+3m)$ without pairs in type (1,10)
(1,2)	$(k,k+3n+1)$, $(k,k+3n+2)$

$$\begin{aligned}F_L=&A(Q_1^2+Q_2^2+Q_3^2+Q_6^2)+B_1(Q_1^2+Q_2^2+Q_3^2+Q_6^2)^2\\&+B_2(Q_1^2Q_3^2+Q_2^2Q_6^2)+B_3Q_3^2Q_6^2+B_4(Q_1^2Q_6^2+Q_2^2Q_3^2)\\&+B_5Q_1^2Q_2^2+C_1(Q_1^2+Q_2^2+Q_3^2+Q_6^2)^3+C_2(Q_1^2+Q_2^2\\&+Q_3^2+Q_6^2)(Q_1^2Q_3^2+Q_2^2Q_6^2)+C_3(Q_1^2+Q_2^2+Q_3^2\\&+Q_6^2)Q_3^2Q_6^2+C_4(Q_1^2+Q_2^2+Q_3^2+Q_6^2)(Q_1^2Q_6^2+Q_2^2Q_3^2)\\&+C_5(Q_1^2+Q_2^2+Q_3^2+Q_6^2)Q_1^2Q_2^2+C_6[(Q_1^2+Q_2^2\\&-Q_3^2)Q_2^2Q_6^2+(Q_1^2+Q_2^2-Q_6^2)Q_1^2Q_3^2+(Q_3^2-Q_6^2)(Q_1^2Q_3^2\\&-Q_2^2Q_6^2)]+C_7[Q_1^4(Q_2^2-Q_3^2-Q_6^2)+Q_2^4(Q_1^2-Q_3^2-Q_6^2)\\&+(Q_3^4-Q_6^4)(Q_1^2-Q_2^2)]+C_8[(Q_1^4-Q_6^4)(Q_2^2+Q_3^2)\\&+(Q_2^4-Q_3^4)(Q_1^2+Q_6^2)]+C_9[(Q_1^4-Q_2^4)(Q_3^2-Q_6^2)\\&+Q_3^4(Q_6^2-Q_1^2-Q_2^2)+Q_6^4(Q_3^2-Q_1^2-Q_2^2)],\end{aligned}\tag{3}$$

$$F_{el}=\frac{\hat{c}_{11}}{2}e_1^2+\frac{\hat{c}_{22}}{2}(e_2^2+e_3^2)+\frac{\hat{c}_{44}}{2}(e_4^2+e_5^2+e_6^2),\tag{4}$$

$$\begin{aligned}F_c=&D_1e_1(Q_1^2+Q_2^2+Q_3^2+Q_6^2)+D_2[\sqrt{3}e_2(Q_6^2-Q_3^2)\\&+e_3\{Q_3^2+Q_6^2-2(Q_1^2+Q_2^2)\}]+D_3[e_2(Q_6^2-Q_3^2+2Q_1^2\\&-2Q_2^2)-\sqrt{3}c_3(Q_3^2+Q_6^2)]+D_4c_6Q_1Q_2,\end{aligned}\tag{5}$$

$$\begin{aligned}F_G=&g_1(Q_{1,x}^2+Q_{2,y}^2)+g_2(Q_{3,x}^2+Q_{2,x}^2+Q_{1,y}^2+Q_{6,y}^2)+g_3(Q_{3,y}^2\\&+Q_{6,x}^2)+g_4Q_{1,y}Q_{2,x}+g_5Q_{1,x}Q_{2,y}.\end{aligned}\tag{6}$$

The symmetry-adapted strain tensor components e_i are defined in terms of the conventional (geometrically linear) strain $\varepsilon_{ij}=\frac{1}{2}[(\partial u_i/\partial x_j)+(\partial u_j/\partial x_i)]$ by the following relations:

$$e_1=\frac{1}{\sqrt{3}}(\varepsilon_{xx}+\varepsilon_{yy}+\varepsilon_{xz}),\tag{7a}$$

$$e_2=\frac{1}{\sqrt{2}}(\varepsilon_{xx}-\varepsilon_{yy}),\tag{7b}$$

$$e_3=\frac{1}{\sqrt{6}}(\varepsilon_{xx}+\varepsilon_{yy}-2\varepsilon_{zz}),\tag{7c}$$

$$e_4=\varepsilon_{xy},\tag{7d}$$

$$e_5=\varepsilon_{yz},\tag{7e}$$

$$e_6=\varepsilon_{xz}.\tag{7f}$$

and the elastic constants $\hat{c}_{ij}$ are given by

$$\hat{c}_{11}=c_{11}+2c_{12},\tag{7g}$$

$$\hat{c}_{22}=c_{11}-c_{12},\tag{7h}$$

$$\hat{c}_{44}=4c_{44}.\tag{7i}$$

Using the variational technique, one obtains the Euler-Lagrange equations, which would generally be six coupled partial differential equations in Q_i and three more equations for the elastic strain

$$\sum_m \frac{\partial}{\partial x_m}\left[\frac{\partial F}{\partial Q_{i,m}}\right]-\frac{\partial F}{\partial Q_i}=0;\tag{8a}$$

$$\sum_{m,\lambda}\frac{\partial}{\partial x_m}\left(\frac{\partial F}{\partial e_\lambda}\frac{\partial e_\lambda}{\partial \varepsilon_{i,m}}\right)=0\quad (m=1,2,3;i,\lambda=1,2,\ldots,6).\tag{8b}$$

where $\varepsilon_{i,m}$ uses the compact Voigt notation. However, two of the components (Q_4,Q_5) of our order parameter are zero.

In the Appendix the coordinate system is rotated 45° around the z axis and the problem becomes quasi-one-dimensional (Q1D). With this Q1D approximation and a space variable x' perpendicular to the OTB, we can write the lattice normal-mode profile for this OTB as $\mathbf{Q}=(Q_1(x'),Q_2(x'),Q_3(x'),0,0,Q_6(x'))$. The forms of the four coupled differential equations resulting from the Euler-Lagrange variation are indicated in the Appendix. The boundary conditions for these equations will depend upon the specific pair of domain states selected.

A twin solution involves two domains of different tetragonal axis. In each of the two domain states, there are two nonzero components of the order parameter (see Table II). The two nonzero components are identical in amplitude. A continuum solution for a twin describes a situation for which the two components with the amplitude Q_0 will vanish gradually across the domain wall instead of disappearing abruptly (discontinuous twin picture) and the other two components increase from zero to Q_0 at the same time. Therefore, the selection of parameters (below) that can reduce the four coupled equations to two coupled equations is not only for computational convenience, it actually reflects the symmetrical nature of these two nonzero components in each domain. They are identical in one side of the domain and gradually decrease inside the domain-wall transition region at the same rate and eventually vanish to zero on the other side of the domain wall at the same time. It is, of course, possible to have the two components vanishing at different rates inside the domain wall, but due to the symmetric nature of the two nonzero components, one would need to motivate where the symmetry-breaking force comes from.

Based on the above considerations, we assume a symmetric relationship of the parameters within the domain wall. This seems reasonable,[16] it conserves the domain wall symmetry of the two order-parameter components and also simplifies the computation. (The four coupled equations can be solved in the same fashion as the two coupled equations, there is not even any new mathematics involved). All essential physical features of a twin solution are reflected in our solution.

The specific orientation twin (I_x, I_y) is chosen to illustrate the procedure and, for the symmetric relationship of mode amplitudes within the domain wall, two coupled equations are then obtained for Q_1 and Q_2 (see Appendix),

$$\frac{(g_1+g_2)}{2}Q_{1,x'x'} = (A+A')Q_1+[4(B_1+B_1')+B_4]Q_1^3 + (4B_1+B_2+B_2'+B_3)Q_1Q_2^2+3(4C_1+C_4)Q_1^5 + (12C_1+2C_2+2C_3+C_4)(Q_1Q_2^4+2Q_2^2Q_1^3),$$

$$\frac{(g_1+g_2)}{2}Q_{2,x'x'} = (A+A')Q_2+[4(B_1+B_1')+B_4]Q_2^3 + (4B_1+B_2+B_2'+B_3)Q_2Q_1^2+3(4C_1+C_4)Q_2^5 + (12C_1+2C_2+2C_3+C_4)(Q_2Q_1^4+2Q_1^2Q_2^3).$$

Using a procedure similar to Refs. 17 and 18 we reduce these two equations to the dimensionless form

$$q_{1,\xi\xi}=\tau_1 q_1-\alpha_1 q_1^3-\alpha_1' q_1 q_2^2+3q_1^5+\beta(2q_1^3q_2^2+q_1q_2^4), \tag{9a}$$

$$q_{2,\xi\xi}=\tau_1 q_2-\alpha_1 q_2^3-\alpha_1' q_2 q_1^2+3q_2^5+\beta(2q_2^3q_1^2+q_2q_1^4), \tag{9b}$$

where

$$\tau_1=\tau+\frac{A'}{A_c},\quad \alpha_1=\frac{4[4(B_1+B_1')+B_4]}{b},$$

$$\alpha_1'=\frac{4(4B_1+B_2+B_2'+B_3)}{b},\quad \beta=\frac{12C_1+2C_2+2C_3+C_4}{4C_1+C_4},$$

and

$$\tau=\frac{T-T_0}{T_c-T_0},\quad b=4B_1+B_4-\left[\frac{4D_1^2}{\hat{c}_{11}}+\frac{4}{\hat{c}_{11}}(D_2+\sqrt{3}D_3)^2\right],\quad A_c=\frac{b^2}{16(4C_1+C_4)}.$$

We also defined the dimensionless order parameter $\mathbf{q}=(q_1,q_2)$ and space variable ξ according to

$$(Q_1,Q_2)=Q_c(q_1,q_2),\quad \gamma\xi=x',$$

with

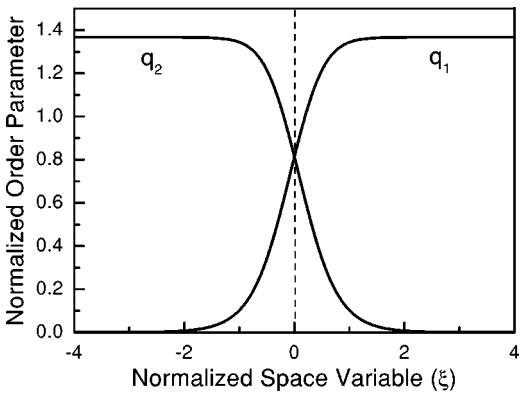

FIG. 2. Solutions of Eqs. (9a,b) with the boundary conditions of Eqs. (11a,b). The parameters chosen for the calculations are $\tau_1=\tau_2=-3$, $\alpha_1=\alpha_1'=4$, and $\beta=5$.

$$\gamma^2=\frac{g_1+g_2}{2}A_c,$$

and

$$Q_c^2=\frac{b}{4(4C_1+C_4)}.$$

The dimensionless order-parameter amplitude q_0 corresponding to Q_0 is given by

$$q_0=[\tfrac{2}{3}(1+\sqrt{1-\tfrac{3}{4}\tau})]^{1/2}. \tag{10}$$

For the I_x-I_y orientational twin, the boundary conditions for q_1 and q_2 are

$$\lim_{\xi\to\infty}(q_1,q_2)=(0,q_0), \tag{11a}$$

$$\lim_{\xi\to\infty}(q_1,q_2)=(q_0,0). \tag{11b}$$

A solution with the choice of $\tau_1=\tau_2=-3$, $\alpha_1=\alpha_1'=4$, and $\beta=5$ is given in Fig. 2. We note that the two values, which characterize the OP, q_1 and q_2, interpenetrate each other in the domain-wall region as expected. The asymptotic values of q_1 and q_2 in the two domains are given in Eqs. (11a,b) above. These profiles represent the relative amplitude variations of the lattice displacement near the domain-wall region. Each lattice will be displaced by an amount determined by the two independent values q_1 and q_2. One may refer to the discrete lattice displacement pattern given in Fig. 3(a) to help understand the continuous displacement pattern.

Note the above simplification of four equations [Eqs. (A3a)–(A3d) and Eqs. (A13a)–(A13d)] to two [Eqs. (A14a, b)] is for the (I_x, I_y) orientational twin. The boundary conditions will change for other orientational twins (see Table V) but we can choose an equivalent wall orientation and position so that the twin-wall structure is symmetrically and energetically equivalent. Shown in Fig. 3(a) is the domain-wall orientation and position that was considered in the procedure developed above, i.e., for the twin wall of the domain pair (3, 2). Notice that the wall passes through the point $(\frac{1}{2},\frac{1}{2},\frac{1}{2})$ and

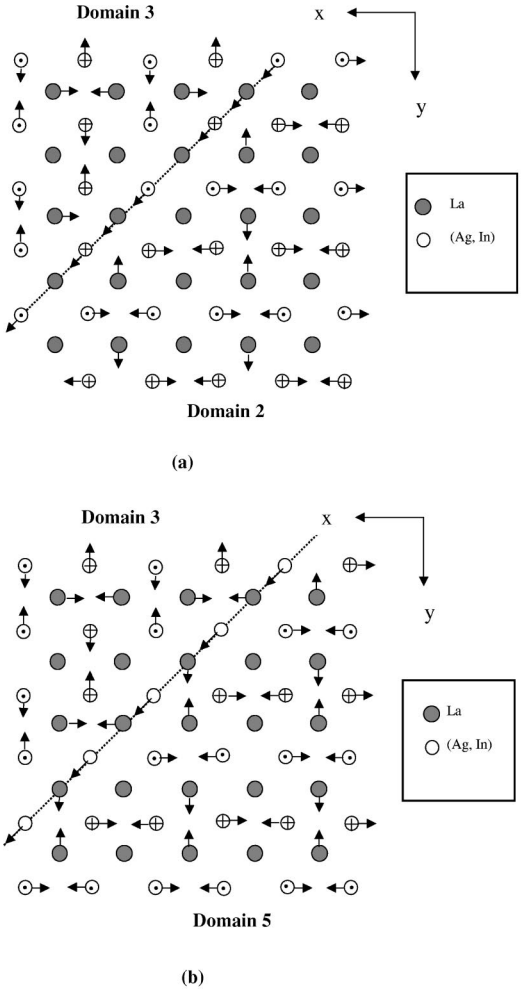

FIG. 3. Lattice displacement patterns for a discontinuous OTB between (a) domains 3 and 2, and (b) domains 3 and 5.

this OTB structure will exhibit the two-dimensional twin symmetry of *Cmm*2. This is a symmetry group that leaves the two domains and the wall invariant, necessarily it is a diperiodic group[19] with translations parallel to the wall. The generating elements of this diperiodic group are $(E|0,0,0)$, $(\sigma_z|0,0,1)$, $(C_{2a}|0,0,0)$, $(\sigma_{db}|0,0,0)$ with the origin at $(\frac{1}{2},\frac{1}{2},\frac{1}{2})$ and basis vectors (0, 0, 2), (2, 2, 0) in terms of the original cubic group. By rotating this entire structure through $(C_{2z}|0,1,0)$ we get the structure given in Fig. 3(b). This domain wall passes through the point $(-\frac{1}{2},\frac{1}{2},\frac{1}{2})$ and will also exhibit the two-dimensional symmetry of *Cmm*2. This twin configuration corresponds to the (I_x,II_y) twin, i.e., the twin wall of domain pair (3,5). The generating elements of the diperiodic group of this structure are $(E|0,0,0)$, $(\sigma_z|0,0,1)$, $(C_{2a}|-1,1,1)$, $(\sigma_{db}-1,1,0)$ with the origin at $(-\frac{1}{2},\frac{1}{2},\frac{1}{2})$ and basis vectors (0, 0, 2), (2, 2, 0) in terms of the original cubic group. The order-parameter profile equations will take the same form if we perform a similar simplification. For example, the reduction from four to two differential equations must use the following conditions: $Q_2=Q_3$, and $Q_1=-Q_6$. The equations and form of the OP profile are their equivalent.

TABLE V. Boundary conditions for orientational twins with order-parameter profile $Q=(Q_1(x'),Q_2(x'),Q_3(x'),0,0,Q_6(x'))$.

Twin of	$x'=-\infty$	$x'=\infty$
I_x-I_y	$(0,Q_0,Q_0,0,0,0)$	$(Q_0,0,0,0,Q_0)$
I_x-II_y	$(0,Q_0,Q_0,0,0,0)$	$(Q_0,0,0,0,0,-Q_0)$
I_x-III_y	$(0,Q_0,Q_0,0,0,0)$	$(-Q_0,0,0,0,0,Q_0)$
I_x-IV_y	$(0,Q_0,Q_0,0,0,0)$	$(-Q_0,0,0,0,0,-Q_0)$
II_x-II_y	$(0,-Q_0,Q_0,0,0,0)$	$(Q_0,0,0,0,0,-Q_0)$
II_x-III_y	$(0,-Q_0,Q_0,0,0,0)$	$(-Q_0,0,0,0,0,Q_0)$
II_x-IV_y	$(0,-Q_0,Q_0,0,0,0)$	$(-Q_0,0,0,0,0,-Q_0)$
III_x-III_y	$(0,Q_0,-Q_0,0,0,0)$	$(-Q_0,0,0,0,0,Q_0)$
III_x-IV_y	$(0,Q_0,-Q_0,0,0,0)$	$(-Q_0,0,0,0,0,-Q_0)$
IV_x-IV_y	$(0,-Q_0,-Q_0,0,0,0)$	$(-Q_0,0,0,0,0,-Q_0)$

Although we have used dimensionless parameters to illustrate the OTB profile, for a specific material, we can obtain the OTB *width* and *energy* using actual GLFE parameters. For the effective GLFE we can estimate the width of the domain wall *w* since below the phase transition $w \simeq 2\sqrt{GC}/|B|$. There is insufficient experimental data to estimate the coefficient *G* accurately. Here *G* denotes an effective gradient coefficient for the material under consideration and quantifies the energy cost needed to create an order-parameter inhomogeneity, an orientational domain wall in the present case. However, based on the parameter estimates given below, if we choose $G\sim 4.0\times 10^7\ \mathrm{J\,m^{-3}\,kg^{-1}}$ we find $w\sim 27.6$ Å, which is approximately four times the cubic lattice parameter.

In Ref. 1, using the available structural and phonon data[20,21] for $LaAg_{1-x}ln_x$ ($x\sim 0.2$), we estimated the coefficients of an effective Landau free energy $F_L=A_0(T-T_0)Q^2+BQ^4+CQ^6$ as $A_0=7.6587\times 10^{23}$ $\mathrm{J\,m^{-5}\,kg^{-1}\,K^{-1}}$ $T_0=120$ K, $B=3.9455\times 10^{70}$ $\mathrm{J\,m^{-7}\,(kg)^{-2}}$, and $C=7.622\times 10^{115}\,\mathrm{J\,m^{-9}\,(kg)^{-3}}$. Similarly we obtained two combinations of gradient coefficients: $g_1+g_2=1.10715\times 10^8$ $\mathrm{J\,m^{-3}\,kg^{-1}}$ and $g_4+g_5=3.96\times 10^7$ $\mathrm{J\,m^{-3}\,kg^{-1}}$.

IV. SUMMARY AND CONCLUSIONS

For a cubic to tetragonal transition an orientational twin consists of two domains that have different tetragonal axes. Elastic compatibility[15,14] requires that the domain wall should lie in particular lattice planes. We have shown that such OTB's produced in an O_h^1–D_{4h}^{17} improper ferroelastic first-order phase transition in $RAg_{1-x}ln_x$ (R=La,Ce,Pr) can be described by a Ginzburg-Landau theory with a six-dimensional order parameter. For a general case, one must numerically solve a system of four-nonlinear-coupled differential equations. This paper provided both the form of the coupled differential equations and the related boundary conditions. The solutions reveal the detailed atomic displacement pattern inside the domain-wall regions. In order to reduce the complication of so many undefined expansion coefficients, we chose a special set of parameters that reduced the four equations to two. The general feature of an

orientational twin can be seen from this simplified solution. The computed OTB profile can be used to predict the attenuation and phase shift associated with the propagation of an ultrasonic pulse in a crystal with a single OTB and its effect on elastic constants.[22] It would be highly desirable to observe the details of this OTB structure in high-resolution electron microscopy.

We used the double coset decomposition and the concept of crystallographically equivalent domain pair classes to identify only one class of OTB's. We gave an example of two different domain pairs (3, 2) and (3, 5), which were crystallographically equivalent. A similar procedure and analysis can also be applied to describe twin boundaries in cubic ($Pm\bar{3}m$) to orthorhombic (*Pmma*) and cubic to trigonal ($P3$) structural transitions observed in the binary AuCd and pseudobinary TiNiM(M=Fe, Al, Cu) shape memory alloys.[5–7]

ACKNOWLEDGMENT

We are grateful to Professor G. R. Barsch for numerous insightful discussions and suggestions. This work was supported in part by NSF Grant No. DNS9704714 and in part by the U.S. Department of Energy under Contract No. W-7405-ENG-36.

APPENDIX: REDUCTION OF VARIATIONAL EQUATIONS

If we make the rotation of the coordinate system around the z axis, the derivatives will be given in terms of the new coordinates as follows:

$$\frac{\partial}{\partial x}=\frac{1}{\sqrt{2}}\frac{1}{\partial x'}+\frac{1}{\sqrt{2}}\frac{\partial}{\partial y'}, \tag{A1a}$$

$$\frac{\partial}{\partial y}=-\frac{1}{\sqrt{2}}\frac{\partial}{\partial x'}+\frac{1}{\sqrt{2}}\frac{\partial}{\partial y'}. \tag{A1b}$$

For a Q1D solution, $\partial/\partial z'=\partial/\partial y'=0$, so that the gradient energy becomes

$$F_G=\tfrac{1}{2}(g_1+g_2)(Q_{1,x'}^2+Q_{2,x'}^2)+\tfrac{1}{2}(g_2+g_3)(Q_{3,x'}^2+Q_{6,x'}^2) -\tfrac{1}{2}(g_4+g_5)Q_{1,x'}Q_{2,x'}, \tag{A2}$$

and

$$\frac{\partial}{\partial x'}\left(\frac{\partial F_C}{\partial Q_{1,x'}}\right)=(g_1+g_2)Q_{1,x'x'}-\tfrac{1}{2}(g_4+g_5)Q_{2,x'x'}, \tag{A3a}$$

$$\frac{\partial}{\partial x'}\left(\frac{\partial F_C}{\partial Q_{2,x'}}\right)=(g_1+g_2)Q_{2,x'x'}-\tfrac{1}{2}(g_4+g_5)Q_{1,x'x'}, \tag{A3b}$$

$$\frac{\partial}{\partial x'}\left(\frac{\partial F_G}{\partial Q_{3,x'}}\right)=(g_2+g_3)Q_{3,x'x'}, \tag{A3c}$$

$$\frac{\partial}{\partial x'}\left(\frac{\partial F_G}{\partial Q_{6,x'}}\right)=(g_2+g_3)Q_{6,x'x'}. \tag{A3d}$$

The Euler-Lagrange equations for the elastic displacement lead to the following conditions for the components of the stress tensor: $\sqrt{2}\sigma_1+\sigma_3+\sqrt{6}\sigma_6=0$, or equivalently, in terms of the symmetry-adapted strain components defined in Eqs. (7a)–(7f)

$$\sqrt{2}\dot{c}_{11}e_1+\sqrt{2}D_1(Q_1^2+Q_2^2+Q_3^2+Q_6^2)+\hat{c}_{22}e_3 +D_2(Q_3^2+Q_6^2-2Q_1^2-2Q_2^2)-\sqrt{3}D_3(Q_3^2+Q_6^2) +\sqrt{6}\dot{c}_{44}e_6+\sqrt{6}D_4Q_1Q_2=0. \tag{A4}$$

Similarly, $\sigma_2=0$, or

$$e_2=\frac{1}{\hat{c}_{22}}[\sqrt{3}D_2(Q_3^2-Q_6^2)+D_3(Q_3^2+2Q_2^2-Q_6^2-2Q_1^2)], \tag{A5}$$

and $\sigma_4+\sigma_5=0$, or

$$e_4=-e_5. \tag{A6}$$

The OTB's (without interface dislocations) must satisfy elastic compatibility constraints. Using the elastic compatibility relation $\varepsilon_{y'z'}=\text{const}=0$ we have

$$e_4-e_5=0. \tag{A7}$$

Thus, from Eqs. (A6) and (A7)

$$e_4=e_5=0. \tag{A8}$$

Another compatibility relation $\varepsilon_{z'z'}=\text{const}$ leads to the following relation:

$$e_1=\sqrt{2}e_3-\left(\frac{2D_1}{\hat{c}_{11}}+\frac{\sqrt{2}(D_2+\sqrt{3}D_3)}{\hat{c}_{22}}\right)Q_0^2. \tag{A9}$$

The last nontrivial compatibility relation $\epsilon_{y'y'}=\text{const}$ gives us

$$\sqrt{2}e_1+e_3-\sqrt{3/2}e_6 =\sqrt{6}\varepsilon_{y'y'}^{\infty}=\left(-\frac{2\sqrt{2}D_1}{\hat{c}_{11}}+\frac{(D_2+\sqrt{3}D_3)}{\hat{c}_{22}}\right)Q_0^2. \tag{A10}$$

From Eqs. (A4), (A9), and (A10) we obtain the elastic stain e_z in terms of the order parameter **Q**

$$e_3=e_3^{\infty}+\left[\frac{\sqrt{2}D_1-2D_2}{2\hat{c}_{11}+\hat{c}_{22}+6\hat{c}_{44}}(Q_0^2-Q_1^2-Q_2^2) +\frac{\sqrt{2}D_1+D_2-\sqrt{3}D_3}{2\hat{c}_{11}+\hat{c}_{22}+6\hat{c}_{44}}(Q_0^2-Q_3^2-Q_6^2) -\frac{\sqrt{6}D_4Q_1Q_2}{2\hat{c}_{11}+\hat{c}_{22}+6\hat{c}_{44}}\right], \tag{A11a}$$

$$e_1 = e_1^{\infty} - \sqrt{2}\left[\frac{\sqrt{2}D_1 - 2D_2}{2\hat{c}_{11}+\hat{c}_{22}+6\hat{c}_{44}}(Q_0^2 - Q_1^2 - Q_2^2) + \frac{\sqrt{2}D_1 + D_2 - \sqrt{2}D_3}{2\hat{c}_{11}+\hat{c}_{22}+6\hat{c}_{44}}(Q_0^2 - Q_3^2 - Q_6^2) - \frac{\sqrt{6}D_4 Q_1 Q_2}{2\hat{c}_{11}+\hat{c}_{22}+6\hat{c}_{44}}\right], \tag{A11b}$$

$$e_6 = \sqrt{6}\left[\frac{\sqrt{2}D_1 - 2D_2}{2\hat{c}_{11}+\hat{c}_{22}+6\hat{c}_{44}}(Q_0^2 - Q_1^2 - Q_2^2) + \frac{\sqrt{2}D_1 + D_2 - \sqrt{3}D_3}{2\hat{c}_{11}+\hat{c}_{22}+6\hat{c}_{44}}(Q_0^2 - Q_3^2 - Q_6^2) - \frac{\sqrt{6}D_4 Q_1 Q_2}{2\hat{c}_{11}+\hat{c}_{22}+6\hat{c}_{44}}\right]. \tag{A11c}$$

These relations are used to eliminate the strains in the equilibrium conditions involving the coupling energy F_c, i.e.,

$$\frac{\partial F_c}{\partial Q_1} = 2(D_1 e_1 - 2D_2 e_3 + 2D_3 e_2)Q_1 + D_4 e_6 Q_2, \tag{A12a}$$

$$\frac{\partial F_c}{\partial Q_2} = 2(D_1 e_1 - 2D_2 e_3 - 2D_3 e_2)Q_2 + D_4 e_6 Q_1, \tag{A12b}$$

$$\frac{\partial F_c}{\partial Q_3} = 2[D_1 e_1 - (\sqrt{3}D_2 + D_3)e_2 + (D_2 - \sqrt{3}D_3)e_3]Q_3, \tag{A12c}$$

$$\frac{\partial F_c}{\partial Q_6} = 2[D_1 c_1 + (\sqrt{3}D_2 + D_3)e_2 + (D_2 - \sqrt{3}D_3)e_3]Q_6, \tag{A12d}$$

where $e_1^{\infty} = -(2D_1/\hat{c}_{11})Q_0^2$ and $e_3^{\infty} = [(D_2 + \sqrt{3}D_3)/\hat{c}_{22}]Q_0^2$.

Now let us consider the Landau part of the equilibrium condition for all four components

$$\frac{\partial F_L}{\partial Q_1} = 2AQ_1 + 4B_1 Q_1 Q_2 + 2B_2 Q_1 Q_3^2 + 2B_4 Q_1 Q_6^2 + 2B_5 Q_1 Q_2^2 + 6C_1 Q_1 Q^4 + 2C_2 Q_1 (Q_1^2 Q_3^2 + Q_2^2 Q_6^2 + Q_3^2 Q^2) + 2C_3 Q_1 Q_3^2 Q_6^2 + 2C_4 Q_1 (Q^2 Q_6^2 + Q_1^2 Q_6^2 + Q_2^2 Q_3^2) + 2C_5 Q_1 (Q_2^2 Q^2 + Q_1^2 Q_2^2) 2C_6 Q_1 [Q_2^2 Q_6^2 + 2Q_1^2 Q_3^2 + Q_2^2 Q_3^2 + Q_3^2 (Q_3^2 - 2Q_6^2)] + 2C_7 Q_1 [2Q_1^2 (Q_2^2 - Q_3^2 - Q_6^2) + Q_2^4 + Q_3^4 - Q_6^4] 2C_8 Q_1 [2Q_1^2 (Q_2^2 + Q_3^2) + Q_2^4 - Q_3^4] + 2C_9 Q_1 [2Q_1^2 (Q_3^2 - Q_6^2) - Q_3^4 + Q_6^4], \tag{A13a}$$

$$\frac{\partial F_L}{\partial Q_6} = 2AQ_6 + 4B_1 Q_6 Q^2 + 2B_2 Q_6 Q_2^2 + 2B_3 Q_6 Q_3^2 + 2B_4 Q_6 Q_1^2 + 6C_1 Q_6 Q^4 + 2C_2 Q_6 (Q_2^2 Q^2 + Q_1^2 Q_3^2 + Q_2^2 Q_6^2) 2C_3 (Q^2 Q_6^2 + Q_3^2 Q_6^2) Q_6 + 2C_4 Q_6 (Q_1^2 Q^2 + Q_1^2 Q_6^2 + Q_2^2 Q_3^2) + 2C_5 Q_6 Q_1^2 Q_2^2 + 2C_6 Q_6 [Q_1^2 Q_2^2 + Q_2^4 - 2Q_1^2 Q_3^2 + 2Q_2^2 Q_6^2 - 2Q_2^2 Q_3^2] + 2C_7 Q_6 [-Q_1^4 - Q_2^4 - 2Q_6^2 (Q_1^2 - Q_2^2)] + 2C_8 Q_6 [-2Q_6^2 (Q_2^2 + Q_3^2) + Q_2^4 - Q_3^4] + 2C_9 Q_6 [Q_2^4 - Q_1^4 + Q_3^4 + 2Q_6^2 (Q_3^2 - Q_1^2 - Q_2^2)], \tag{A13b}$$

$$\frac{\partial F_L}{\partial Q_2} = 2AQ_2 + 4B_1 Q_2 Q^2 + 2B_2 Q_2 Q_6^2 + 2B_4 Q_2 Q_3^2 + 2B_5 Q_{21}^2 + 6C_1 Q_2 Q^4 + 2C_2 Q_2 (Q_6^2 Q^2 + Q_1^2 Q_3^2 + Q_2^2 Q_6^2) + 2C_3 Q_2 Q_3^2 Q_6^2 + 2C_4 Q_2 (Q_3^2 Q^2 + Q_1^2 Q_6^2 + Q_2^2 Q_3^2) + 2C_5 Q_2 (Q_1^2 Q^2 + Q_1^2 Q_2^2) + 2C_6 Q_2 (2Q_2^2 Q_6^2 + Q_6^2 Q_1^2 + Q_1^2 Q_3^2 - 2Q_3^2 Q_6^2 + Q_6^4) + 2C_7 Q_2 [\dot{Q}_1^4 + 2Q_2^2 (Q_1^2 - Q_3^2 - Q_6^2) - Q_3^4 + Q_6^4] + 2C_8 Q_2 [Q_1^4 - Q_6^4 + 2\dot{Q}_2^2 (Q_1^2 + Q_6^2) + 2C_9 Q_2 [2Q_2^2 (Q_6^2 - Q_3^2) - Q_3^4 - Q_6^4], \tag{A13c}$$

$$\frac{\partial F_L}{\partial Q_3} = 2AQ_3 + 4B_1 Q_3 Q^2 + 2B_2 Q_3 Q_1^2 + 2B_3 Q_3 Q_6^2 + 2B_4 Q_3 Q_2^2 + 6C_1 Q_3 Q^4 + 2C_2 Q_3 (Q_1^2 Q^2 + Q_1^2 Q_3^2 + Q_2^2 Q_6^2) + 2C_3 Q_3 (Q_6^2 Q^2 + Q_3^2 Q_6^2) + 2C_4 Q_3 (Q_2^2 Q^2 + Q_1^2 Q_6^2 + Q_2^2 Q_3^2) + 2C_5 Q_3 Q_1^2 Q_2^2 + 2C_6 Q_3 (-2Q_2^2 Q_6^2 + Q_1^4 + Q_1^2 Q_2^2 - 2Q_1^2 Q_6^2 + 2Q_1^2 Q_3^2) + 2C_7 Q_3 (Q_1^4 - Q_2^4 + 2Q_1^2 Q_3^2 - 2Q_2^2 Q_3^2) + 2C_8 Q_3 (Q_1^4 - Q_6^4 - 2Q_1^2 Q_3^2 + 2Q_3^2 Q_6^2) + 2C_9 Q_3 [Q_1^4 - Q_2^4 + Q_6^4 + 2Q_3^2 (Q_6^2 - Q_1^2 - Q_2^2)], \tag{A13d}$$

where $Q^2=(Q_1^2+Q_2^2+Q_3^2+Q_6^2)$.

Substituting Eqs. (A3), (A6), (A11), (A12) and (A13) into Euler's equilibrium condition, we find four coupled differential equations for the four nonzero components of the OP. The boundary conditions, given in Table V, are determined for a specific pair of domain states.

These four coupled nonlinear differential equations can only be solved numerically. For the orientation twin (I_x, I_y), we choose $Q_1=Q_6$ and $Q_2=Q_3$ to illustrate the general features of an OTB solution. This choice reduces the four coupled equations to two equations. From Table V, we note that this condition is always true in a single-domain state, i.e., at $x'=\pm\infty$. From Eqs. (A13) we see this can be generally true only when $B_3=B_5$, $C_3=C_5$, and $C_6=C_7=C_8=C_9=0$. In addition, the coupling coefficients must satisfy $D_4=0$ and $D_3=\sqrt{3}D_2$, and the gradient coefficients must satisfy the following conditions: $g_1=g_3$ and $g_4+g_5=0$. With these conditions Eqs. (A12) can be simplified to

$$\frac{\partial F_c}{\partial Q_1}=\left\{2\left[D_1e_1^{\infty}-2D_2e_3^{\infty}-\frac{2(\sqrt{2}D_1-2D_2)^2Q_0^2}{2\hat{c}_{11}+\hat{c}_{22}+6\hat{c}_{44}}\right]+\left[\frac{4(\sqrt{2}D_1+2D_2)(\sqrt{2}D_1-2D_2)}{2\hat{c}_{11}+\hat{c}_{22}+6\hat{c}_{44}}-\frac{48D_2^2}{\hat{c}_{22}}\right]Q_1^2+\left[\frac{4(\sqrt{2}D_1+2D_2)(\sqrt{2}D_1-2D_2)}{2\hat{c}_{11}+\hat{c}_{22}+6\hat{c}_{44}}+\frac{48D_2^2}{\hat{c}_{22}}\right]Q_2^2\right\}Q_1, \tag{A14a}$$

$$\frac{\partial F_c}{\partial Q_2}=\left\{2\left[D_1e_1^{\infty}-2D_2e_3^{\infty}-\frac{2(\sqrt{2}D_1-2D_2)^2Q_0^2}{2\hat{c}_{11}+\hat{c}_{22}+6\hat{c}_{44}}\right]+\left[\frac{4(\sqrt{2}D_1+2D_2)(\sqrt{2}D_1-2D_2)}{2\hat{c}_{11}+\hat{c}_{22}+6\hat{c}_{44}}-\frac{48D_2^2}{\hat{c}_{22}}\right]Q_2^2+\left[\frac{4(\sqrt{2}D_1+2D_2)(\sqrt{2}D_1-2D_2)}{2\hat{c}_{11}+\hat{c}_{22}+6\hat{c}_{44}}+\frac{48D_2^2}{\hat{c}_{22}}\right]Q_1^2\right\}Q_2, \tag{A14b}$$

and the equilibrium conditions, Eqs. (A13), are reduced to two-coupled equations for Q_1 and Q_2, given in Sec. III just before Eqs. (9).

The corresponding parameters A_1', B_1', and B_2' are given by

$$A'=D_1e_1^{\infty}-2D_2e_3^{\infty}-\frac{2(\sqrt{2}D_1-2D_2)^2}{2\hat{c}_{11}+\hat{c}_{22}+6\hat{c}_{44}}Q_0^2, \tag{A15a}$$

$$B_1'=\frac{(\sqrt{2}D_1+2D_2)(\sqrt{2}D_1-2D_2)}{2(2\hat{c}_{11}+\hat{c}_{22}+6\hat{c}_{44})}-\frac{6D_2^2}{\hat{c}_{22}}, \tag{A15b}$$

$$B_2'=\frac{4(D_1^2-2D_2^2)}{2\hat{c}_{11}+\hat{c}_{22}+6\hat{c}_{44}}+\frac{24D_2^2}{\hat{c}_{22}}. \tag{A15c}$$

[1] W. Cao, A. Saxena, and D. M. Hatch, Phys. Rev. B **64**, 024106 (2001).

[2] A. Saxena, G. R. Barsch, and D. M. Hatch, Phase Transitions **46**, 89 (1994). Note that the 11th invariant of sixth order [see Eq. (3a) in Sec. II] was inadvertently left out in Tables 4a and 4b of this reference.

[3] D. M. Hatch, P. Hu, A. Saxena, and G. R. Barsch, Phys. Rev. Lett. **76**, 1288 (1996).

[4] H. T. Stokes and D. M. Hatch, *Isotropy Subgroups of the 230 Crystallographic Space Groups* (World Scientific, Singapore, 1988).

[5] T. Ohba, Y. Emura, S. Miyazaki, and K. Otsuka, Mater. Trans., JIM **31**, 12 (1990).

[6] G. R. Barsch, T. Ohba, and D. M. Hatch, Mater. Sci. Eng., A **273–275**, 161 (1999).

[7] G. R. Barsch, Mater. Sci. Forum **327–328**, 367 (2000).

[8] C. J. Bradley and A. P. Cracknell, *The Mathematical Theory of Symmetry in Solids* (Clarendon, Oxford, 1972).

[9] D. M. Hatch, J. S. Kim, and H. T. Stokes, Phys. Rev. B **33**, 6196 (1986).

[10] M. Guymont, Phys. Rev. B **18**, 5385 (1978).

[11] R. Dirl, P. Zeiner, B. L. Davies, and V. Janovec, Acta Crystallogr., Sect. A: Found. Crystallogr. **53**, 456 (1997).

[12] V. Janovec, Czech. J. Phys., Sect. B **22**, 974 (1972).

[13] V. Janovec, W. Schranz, H. Warhanek, and Z. Zikmund, Ferroelectrics **98**, 171 (1989).

[14] J. Fousek and V. Janovec, J. Appl. Phys. **30**, 135 (1969).

[15] J. Sapriel, Phys. Rev. B **12**, 5128 (1975).

[16] Note that high resolution TEM observation of domain walls in other materials, e.g., ferroelectric $PbTiO_3$, justifies this assumption. S. Stemmer, S. K. Streilfer, F. Ernst, and M. Rühle, Philos. Mag. A **71**, 713 (1995).

[17] W. Cao and G. R. Barsch, Phys. Rev. B **41**, 4334 (1990).

[18] W. Cao and L. E. Cross, Phys. Rev. B **44**, 5 (1991); Ferroelectrics **157**, 19 (1994).

[19] D. M. Hatch and H. T. Stokes, Phase Transitions **7**, 87 (1986).

[20] J. Maetz, M. Müllner, H. Jex, W. Assmus, and R. Takke, Z. Phys. B **37**, 39 (1980).

[21] K. Knorr, B. Renker, W. Assmus, B. Lüthi, R. Takke, and H. J. Lauter, Z. Phys. B: Condens. Matter **39**, 151 (1980).

[22] N. A. Sujatha and G. R. Barsch, in *Twinning in Advanced Materials*, edited by M. H. Woo and M. Wuttig (The Minerals, Metals, and Materials Society, Warrendale, PA, 1994), p. 247.